Received: 8 November 2019 | Revised: 10 February 2020 | Accepted: 8 March 2020

DOI: 10.1002/jbm.b.34608

ORIGINAL RESEARCH REPORT

Society For Biomaterials | WILEY

A novel crosslinker-free technique toward the fabrication of collagen microspheres

Colten Snider[1] | Mitch Bellrichard[2] | Amber Meyer[3] | Raghuraman Kannan[1,4] | Dave Grant[1] | Sheila Grant[1]

[1]Department of Biomedical, Biological & Chemical Engineering, University of Missouri, Columbia, Missouri

[2]Department of Veterinary Pathology, University of Missouri, Columbia, Missouri

[3]Department of Materials Science and Engineering, Missouri University Science & Technology, Rolla, Missouri

[4]Department of Radiology, University of Missouri, Columbia, Missouri

Correspondence
Sheila Grant, Department of Biomedical, Biological & Chemical Engineering, University of Missouri, Columbia, MI, USA.
Email: grantsa@missouri.edu

Abstract

Injectable collagen microspheres (CMs) have the potential to be an excellent tool to deliver various modulatory agents or to be used as a cellular transporter. A drawback has been the difficulty in producing reliable and spherical CMs. A crosslinker-free method to fabricate CMs was developed using liquid collagen (LC) in a water-in-oil emulsion process with varying concentrations of surfactant span-80. Different emulsion times of up to 16-hr were utilized to produce the CMs. Visual microscopy and scanning electron microscopy were utilized to determine the morphology of the CMs. To determine the fibril nature of the CMs, focus ion beam milling, energy dispersive spectroscopy, and Fourier Transformation-Infrared spectroscopy were performed. A cell biocompatibility study was performed to assess the biocompatibility of the CMs. The results demonstrated that consistent spherical CMs were achievable by changing the span-80 concentration. The CMs were fibrilized not only at the surface, but also at the core. Both the 1- and 16-hr emulsion time demonstrated biocompatibility and it appeared that the cells preferentially adhered to the CMs. This crosslinker-free method to fabricate CMs resulted in spherical, stable, biocompatible CMs, and could be an excellent technique for multiple tissue engineering applications.

KEYWORDS

collagen, emulsification, microbead, microparticle, microsphere

1 | INTRODUCTION

Recent advances in the field of musculoskeletal deficiencies, histogenesis, and chondro/osteoinduction are mainly attributed to the utilization of naturally occurring collagen as fillers (Glowacki & Mizuno, 2008). Collagen is the most abundantly found protein in the human body, with collagen Type I, II, and III composing 80–90% of all collagen (Uzman, 2001). The triple helix of Type I collagen is composed of three peptide chains that have α1 and α2 subunits, having a characteristic repeating X-Y-Glycine sequence, with X and Y most commonly being proline and hydroxyproline, respectively (Shoulders & Raines, 2009). A single triple helix conforms with two α1 subunits and one α2 subunit contributing to its design as an integral structural component and thus allowing collagen to be an excellent candidate for biomaterial applications (Bella, Eaton, Brodsky, & Berman, 1994).

Collagen is also commonly used in biomedical applications due to its excellent biocompatibility and is biodegradable with no harsh byproducts (Parenteau-Bareil, Gauvin, & Berthod, 2010). Collagen can be processed in many forms and shapes using various processes including casting, molding (Savolainen et al., 1988), electrospinning (Chen, Chang, & Chen, 2008), and 3D printing (Mozdzen, Rodgers, Banks, Bailey, & Harley, 2016). While these processes can result in many different shapes and forms of the collagen structure, for tissue engineering applications, it is highly desirable for the collagen materials to be injectable as it allows minimal invasive surgeries, faster healing times, and less inflammation. Among all shapes, spheres of

collagen, as microspheres, have attracted special attention due to their injectable characteristics (Nagai et al., 2010).

Collagen microspheres (CMs) have been utilized as injectable in tissue applications for recapitulation of cartilage (Li, Cheng, Cheung, Chan, & Chan, 2014), bone (Mumcuoglu et al., 2018), blood vessel (Nagai et al., 2010), and intervertebral disc development (Yuan, Leong, & Chan, 2011). In addition, the microspheres have also been used as a drug transporter for proteins such as bovine serum albumin (Chan, So, & Chan, 2008), histone (Chan et al., 2008), bone morphogenetic protein 2 (Mumcuoglu et al., 2018), vascular endothelial growth factor (Nagai et al., 2010), and transforming growth factor beta-3 (Mathieu et al., 2014). Furthermore, CMs have not only been utilized to entrap and carry various proteins, but have also been used to entrap and carry cells like chondrocytes and mesenchymal stem cells (MSCs; Li et al., 2014; Liu, Lin, Li, Fan, & Zhang, 2015). For example, an interesting study by Li et al. (2014). describes the entrapment of undifferentiated and chondrogenic predifferentiated MSC within CMs into an osteochondral defect rabbit model. The authors have demonstrated that regardless of whether the MSCs were undifferentiated or differentiated, the higher cell density resulted in better histological scores. Further, the study showed that undifferentiated and predifferentiated MSCs at high cell densities produced hyaline cartilage. Even though there have been many biomedical applications for CMs, the fabrication of CMs is cumbersome and labor-intensive; current fabrication procedures require crosslinkers during emulsification which can lead to cytotoxicity or pipetting cycles that are time-consuming and produce noninjectable microspheres (Li et al., 2014; Yuan et al., 2011).

The current CMs fabrication procedures commonly utilized micropipetting of collagen or emulsion. For example, neutralized Type I rat tail collagen was micropipetted onto a parafilm lined Petri dish; the collagen gelled into a spherical form under physiological temperatures and conditions (Li et al., 2014; Yuan et al., 2011). This technique suffers disadvantages as it requires individual pipetting cycles to obtain CMs, which is time-consuming and laborious. More importantly, the technique yields microspheres of different sizes ranging from 300 to 1,000 μm. Other researchers have worked on the fabrication to overcome this disadvantage; Nagai et al. (2010) utilized a water-in-oil emulsion process to fabricate CMs. Commonly, a collagen solution is added to an oil emulsion and allowed to stir for a set amount of time. Preceding work have used various oils such as corn oil, PDMS, paraffin oil, olive oil, paraffin/olive oil, and perfluorinated oil with surfactants such as tween-20, span-20, span-80, and have also used a range of emulsion rates ranging from 300 to 1,200 rpm that have all contributed to changing the average CM diameters (Chan et al., 2008; Liu et al., 2015; Mathieu et al., 2014; Mumcuoglu et al., 2018; Nagai et al., 2010; Yang & Wang, 2014). By varying these parameters, prior publications have fabricated CMs of various sizes from several microns to 300 μm. One vital factor to consider is the use of crosslinking agents in forming CMs. These agents are used during the emulsification process to form stable CMs. Chemical crosslinking agents used to fabricate CMs with good stability include glutaraldehyde (Chowdhury & Mitra, 1999; Wu et al., 2004) and EDC/NHS (1-Ethyl-3-[3-dimethylaminopropyl]carbodiimide hydrochloride)/*N*-hydroxysuccinimide (Matsuhashi, Nam, Kimura, & Kishida, 2015; Nagai et al., 2010; Yang & Wang, 2014). A disadvantage of the use of traditional chemical crosslinker glutaraldehyde is that they have long been shown to have cytotoxic effects (Gough, Scotchford, & Downes, 2002; Sung, Huang, Huang, & Tsai, 1999). In addition, the use of chemical crosslinkers can also effect cellular adhesion to Type I collagen. Bax et al. (2017) describes the use of EDC/NHS crosslinking on Type I collagen inhibiting native-like cellular adhesion. They have proposed that the use of EDC/NHS crosslinking modifies the carboxylic acid groups on collagen altering divalent cation-dependent cell adhesion to cation-independent cell adhesion.

We have investigated CMs using a prefibrilized, liquid collagen (LC) solution to avoid the use of traditional crosslinking agents to maintain CM stability. LC was initially developed as a crosslinker-free soft tissue filler which fibrilizes in situ (Devore et al., 2016). Previous studies have suggested that LC remains in a prefibrilized state due to the inclusion of ethylenediaminetetraacetic acid (EDTA) which surrounds the collagen fibrils preventing the formation of a triple helix leading to fibrillization (Devore et al., 2016). Another possible explanation proposed is multiple ionic interactions occurring upon different regions along the individual collagen fibrils preventing fibrillization. Fibrillization of the collagen occurs when it is introduced into physiological tissue fluids resulting in the displacement of either the EDTA or the ions allowing for the formation of individual fibrils into its triple helix structure. Heat can also trigger the fibrillization of LC due to the collagen fibrils energetically preferring to fibrilize. The transition from liquid to a fibrilized network is visually evident as the LC transition from a clear liquid to a semi-solid opaque material maintaining the structural form. The advantages of utilizing LC include no toxic effects shown in vivo, and its inherent resistance to collagenase digestion, native tissue in-growth in vivo, and vascularization in vivo (Devore et al., 2016).

LC is an excellent material to use in the fabrication of CMs with a water-in-oil emulsion due to its ease of fibrillization under heated temperatures, reliving the need for a crosslinker. Here we describe a novel method to fabricate crosslinker-free CMs using span-80 and olive oil emulsion. Span-80, a surfactant, was utilized to manipulate the CM diameter, and fibrillization of the CMs was achieved by emulsification at 35°C due to the energetically favorable reaction within the solution. The results demonstrated that reproducible CMs were achieved and the size ranges can be manipulated by utilizing different concentrations of surfactant. The CMs demonstrated biocompatibility and stability over time. It is expected that these CMs will be able to serve as an injectable carrier of biomodulatory agents like stem cells, proteins, and drugs.

2 | MATERIALS AND METHODS

2.1 | Fabrication of LC

Porcine collagen Type I (10 mg/ml, Sunmax Biotechnology, Taiwan) was precipitated using 1.04 M sodium chloride (NaCl, ≥99.0%, Sigma Aldrich, MO). The precipitated collagen solution was then centrifuged at 3,500 rpm for 15 min. A white collagen pellet was formed at the

bottom of the tube and the supernatant was poured off leaving a 150 mg collagen pellet. Fifteen ml of 0.5 M glacial acetic acid (≥99.7%, Fisher Chemical, KS) was added to the collagen pellet and allowed to sit overnight at room temperature to let the collagen pellet dissolve. The collagen/acetic acid solution was then placed in a 15 ml, 10 kDa molecular weight cutoff dialysis cassette (Thermo Scientific, IL) and immersed in an ethylenediaminetetraacetic acid (35 mM, EDTA, Fisher Chemical, KS)/H_2O solution with a pH of 7.5 using sodium hydroxide (10 N, NaOH, Ricca Chemical Co., TX) (Devore et al., 2016). The pH of the EDTA solution was checked and maintained at 7.5 daily until the pH no longer fluctuated from 7.5. The collagen solution was then removed and pH was tested to ensure it was set at 7.5.

2.2 | Fabrication of collagen microspheres

Fifty ml of olive oil (Sigma Aldrich) and correlating volume of span-80 (Sigma Aldrich) was added to a 100 ml round bottom flask. A 4 cm stir bar was added to the flask and placed on a stir/hot plate and set to 1,150 rpm. The emulsion was allowed to equilibrate for 10 min. After 10 min, 1 ml of the LC solution was added dropwise using an 18-gauge plastic cannula. One hour after the LC addition, the stir plate temperature was set to 35°C and allowed to stir for up to 16-hrs. Preliminary studies show fibril formation occurring 1 min after LC was added to 37°C olive oil, data not shown. After the emulsion time was reached the collagen/oil solution was poured into a 50 ml centrifuge tube and centrifuged at 5000 rpm for 5 min. The oil was then removed and 25 ml 50% acetone (Fisher Chemical, KS) and 100 μl tween-20 (Sigma Aldrich) was added to the tube to wash the CMs. The solution was vortexed for 1 minute and sonicated for 3 min. The solution was then centrifuged at 5,000 rpm for 5 min. The sample was washed three times using 50% acetone and tween-20 and then was washed three times using ×1 PBS (Sigma Aldrich). The CMs were stored in 15 ml ×1 PBS and placed in a 4°C refrigerator. They have been shown to remain stable for at least 10 months.

2.3 | CM diameter characterization

To determine the effects of the emulsion time and surfactant concentration on CM diameter, an inverted light microscope (IX50, Olympus, PA) with a ×4 objective was utilized to examine the CMs. A 1:1 ratio of CMs to Trypan blue (0.4%, Sigma Aldrich) dye was added to help visualize CMs under the microscope. Images were captured using SPOT software and CM diameters were measured using ImageJ. At least 100 CM diameters were collected per group and analyzed.

2.4 | Electron microscopy characterization

CM morphology was studied using a scanning electron microscope (SEM) (Scios DualBeam, Thermo Scientific, MA), 5–15 kV was used to image the sample. Samples were placed in a fixative solution of 100 nM sodium cacodylate, 2% glutaraldehyde, and 2% paraformaldehyde (provided by the University of Missouri Electron Microscopy Core) for 30 min and washed three times with H_2O. Samples were then placed on carbon tape, and the liquid was allowed to evaporate for 1-hr at 40°C prior to imaging for hydrated imaging. Critical point drying (CPD) was also used to image CMs. For CPD, samples were negative stained with osmium and coated with platinum once fixed on carbon tape. Focused ion beam (FIB) milling was utilized to create a cross-section to determine the fibril structure of the core of the CMs. A gallium ion beam was used during FIB milling. Additionally, energy-dispersive X-ray spectroscopy (EDS) was conducted on the CMs to identify the elemental composition of the CMs.

2.5 | FTIR

Fourier-transform infrared spectroscopy (FTIR) was performed to verify the collagen fibril formation in the CMs. An ATR-FTIR (Nicolet 6,700, Thermo Scientific, MA) was utilized. Ten replicates from each sample were analyzed by averaging 32 scans per sample at a resolution of 4 cm^{-1} at room temperature. Samples were prepared by storage in a −20°C refrigerator for 24 hr and lyophilizing using a Labconco FreeZone-1 for 24 hr.

2.6 | Cell biocompatibility

Cell biocompatibility testing was performed to verify the cellular viability of L-929 fibroblast cells (ATCC, VA) with CMs. L-929 murine fibroblast cells were cultured at 37°C and 5% CO_2 in Eagle's Minimum Essential Medium (ATCC, VA) supplemented with horse serum (10%, ATCC, VA) and penicillin–streptomycin (200 U/ml, ATCC, VA). Cells were subcultured and given fresh cell media as needed. All assays were performed in a biological safety cabinet under sterile conditions.

Cell proliferation reagent WST-1 (Sigma Aldrich) was utilized to assess the biocompatibility of the CMs. In this assay, tetrazolium salts were added to wells containing cells and CMs. The CMs were incubated in cell media for 24 hr at 37°C before being added to a 96 well plate. 0.75×10^4 L-929 murine fibroblasts/well were added to a 96 well plate and 24 hr later CMs were added to the cell seeded well plate. Half of the medium in each well was replaced after 72 hr. At the terminal time point, WST-1 reagent was added to each well and the plates were incubated at 37°C for 4 hr. After 4 hr, the media was removed from each well and absorbance readings were taken at 450 nm, with 600 nm filter, using a spectrofluorometer plate reader (Cytation 5, BioTek, VT). L-929 fibroblasts with no CM scaffold served as the 100% viability baseline.

3 | RESULTS

3.1 | Influence of surfactant concentration on microsphere diameter

To understand the influence of span-80 on the size of CMs, we performed the fabrication in various concentrations of span-80.

Specifically, we varied the concentrations from 0 to 0.50% (v/v). The mean, standard deviation, median, and size range of each concentration is also shown in Table 1. The average diameter and standard deviation of the CMs decreased with the increase in concentrations of span-80 from 92.7 ± 44.1 um with 0% span-80 to 22.7 ± 12.9 um with 0.35% span-80. Using a one-way analysis of variance (ANOVA) with a pairwise Tukey test ($p < .05$), a difference in the average diameter of CMs was observed between 0.02%, 0.10%, 0.20%, and 0.35% span-80 concentrations.

Figure 1 includes ×4 light microscope images of CMs, which were dyed with trypan blue to increase visibility. The figures demonstrate an increase in span-80 concentration to the reaction mixture up to 0.35%, lead to a decrease in particle size, as evidenced by the figures.

TABLE 1 Mean, standard deviation, median, and size range of counted CMs for each concentration of span-80 emulsion

Span-80 concentration (v/v%)	Mean (μm)	Standard deviation (±)	Median (μm)	Size range (μm)
0	92.7	44.1	86.3	18.0–222.0
0.02	86.1	40.0	83.0	18.9–188.3
0.10	60.3	29.6	57.2	18.1–139.3
0.20	35.9	13.6	33.3	18.4–85.3
0.35	22.7	12.9	20.8	8.0–85.2

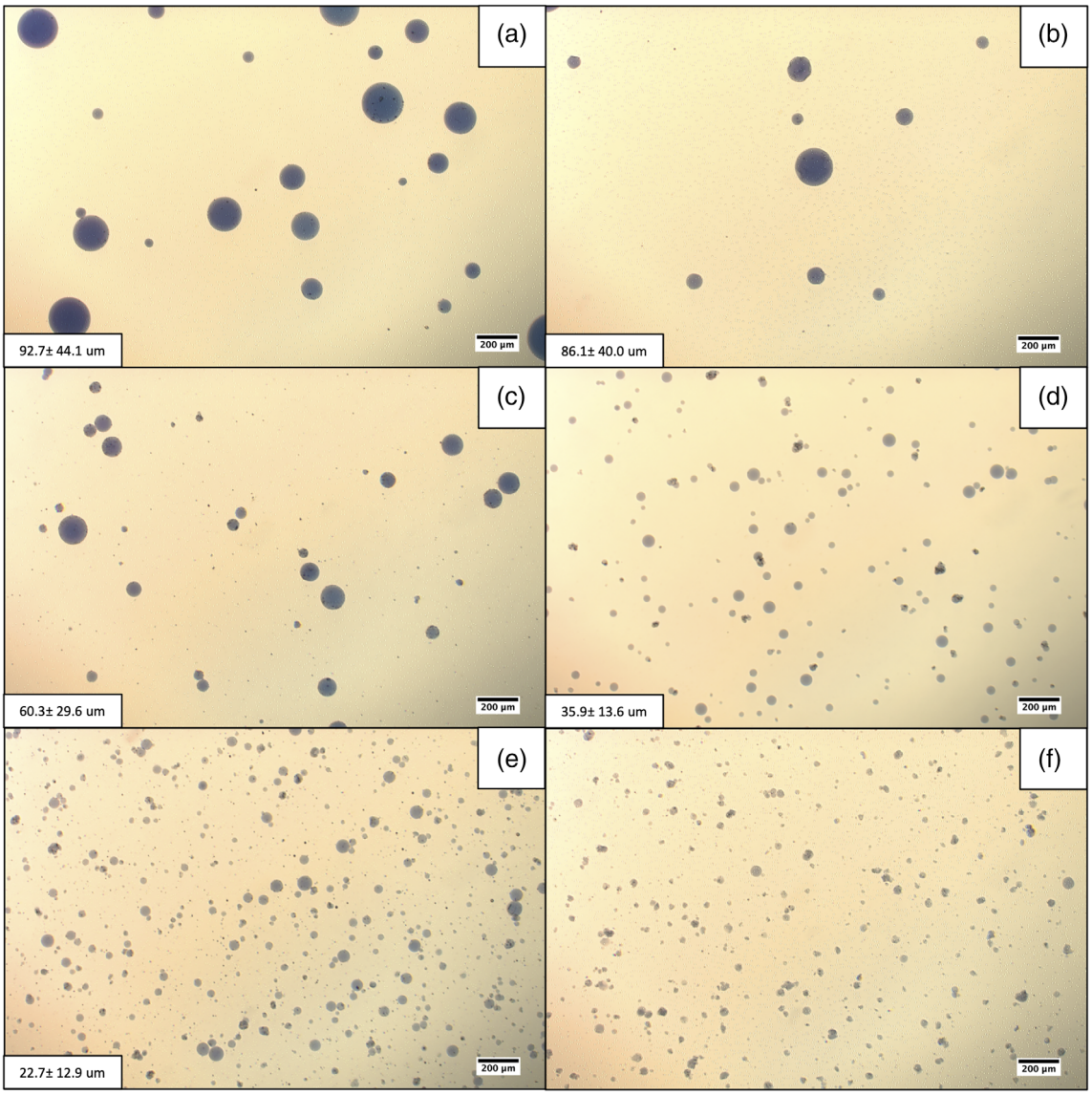

FIGURE 1 ×4 light microscope images of 1-hr emulsion CMs with (a) 0% span-80, (b) 0.02% span-80, (c) 0.10% span-80, (d) 0.20% span-80, (e) 0.35% span-80, and (f) 0.50% span-80; Scale bar = 200 um

However, the particle size did not significantly decrease after increasing the concentration of span-80 over 0.35% (v/v). Interestingly, upon increasing the concentrations of span-80 emulsion to 0.50% (v/v), the spherical morphology of the CMs was no longer maintained (Figure 1f). Based on the result, we determined that 0.35% (v/v) of span-80 in the formulation is considered to optimal concentration for generating uniform size CMs.

3.2 | SEM and EDS characterization

The spherical morphology of a hydrated, 1-hr CM emulsion is observed in Figure 2a of the SEM micrograph. Collagen fibrils were not immediately evident based on the surface morphology of the CM. FIB milling was utilized to mill half of the of the CM, as shown in Figure 2b–h, to show the cross-section to reveal the morphology of the CM core. A progression from initial milling to fully milled CM (Figure 2b–h) took a total time of 29 min with a 3 nA current. After initial milling of the sphere, collagen fibrils were revealed. Further milling, as shown in Figure 2c–f, continued to reveal the collagen fibrils throughout the CM. A collagen network can be seen in Figure 2h cross-section along with white salt crystals.

Figure 3a is an SEM micrograph of an 8-hr CM emulsion that has been fixed and critically point dried. Collagen fibrils appear to be evident on the surface of the CM in Figure 3a. Figure 3b is a magnified view of the CM within the highlighted green box in Figure 3a. Visually

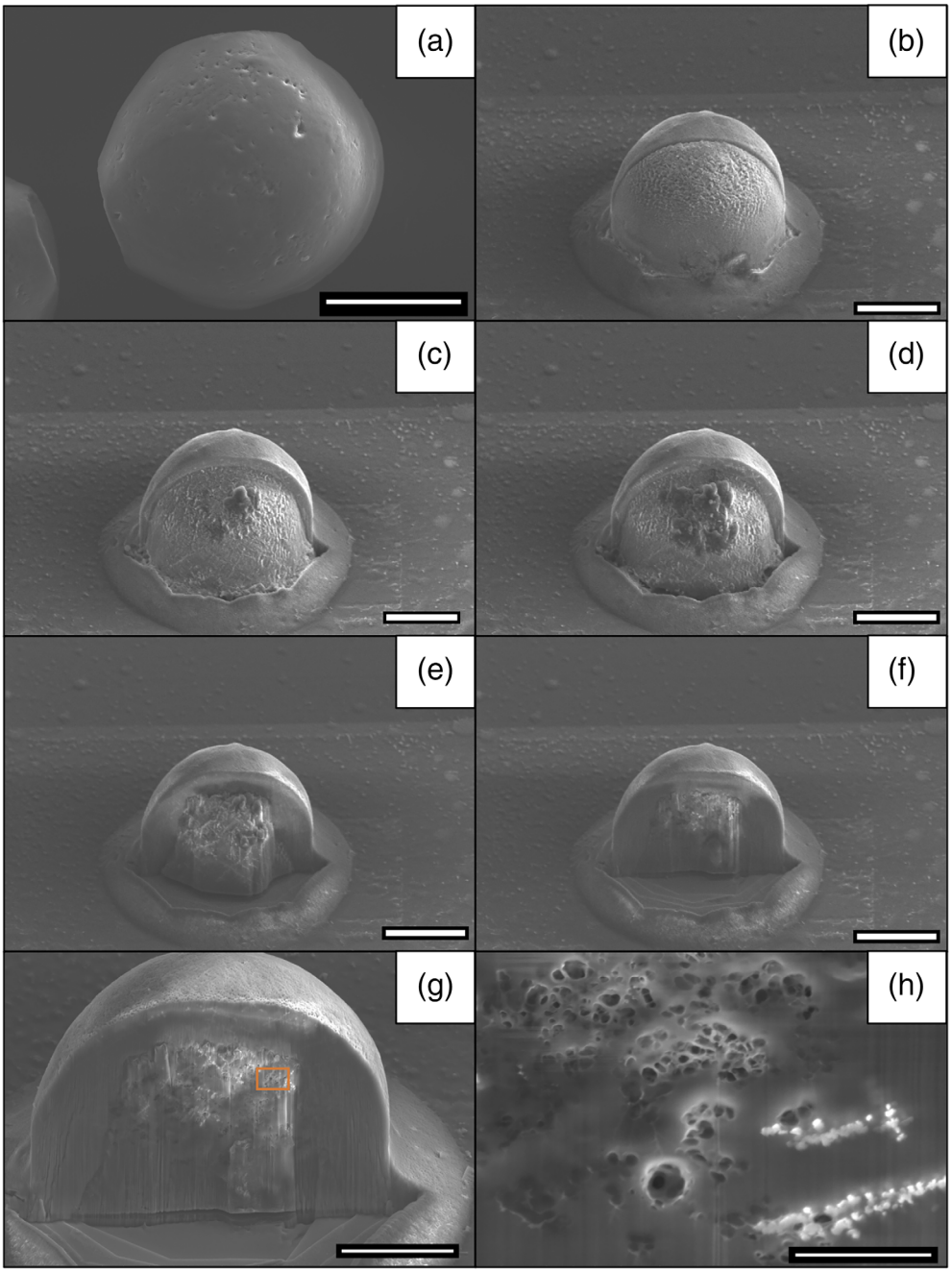

FIGURE 2 SEM micrograph of a CM emulsified for 1-hr and milled using gallium FIB milling. (a) A CM prior to milling. (b)-(f) Images taken during milling requiring 29 min with a 3 nA current. (g)A cross section of the core of the CM. (h)A high magnification image of the cross section from the orange box in (g); Scale bar = 5 um

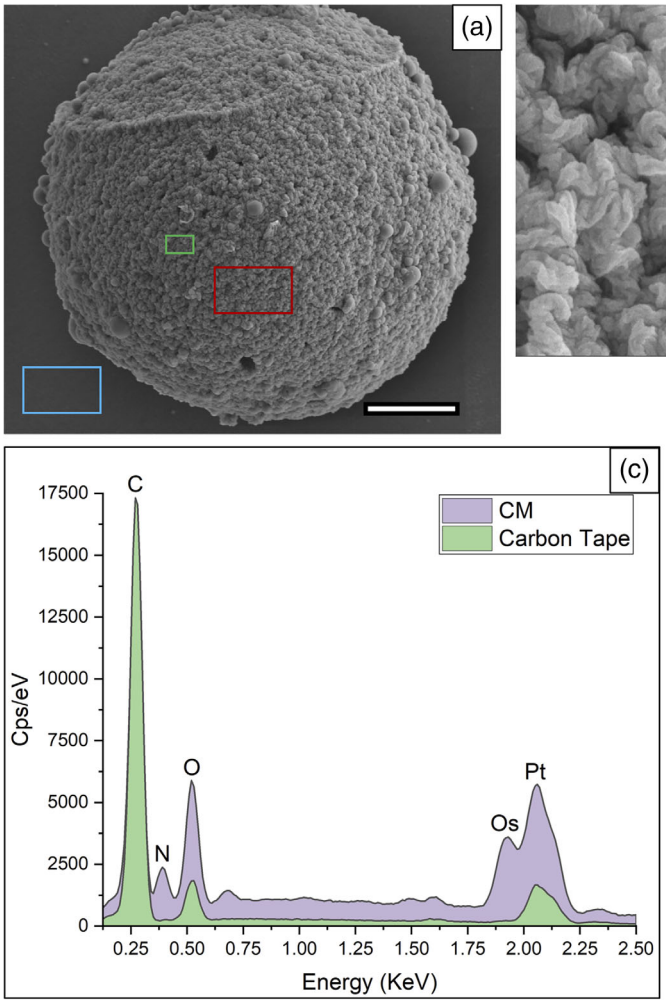

FIGURE 3 SEM micrograph of a CM emulsified for 8-hrs (a) ×9,000 magnification of CM, (b) ×80,000 magnification of CM within the region of the red square from image (a), (c) EDS spectra acquired from the CM (red box in (a)) and on carbon tape (blue box in (a)); Scale bar = 5 um

these fibrils appear to be a mature fibrilized network maintaining a spherical structure. Figure 3c is an EDS spectrum acquired on the surface of the CM (red box) and the carbon tape (blue box) as a background spectra. A strong nitrogen signal was acquired from the CM relative to the carbon tape background. A nitrogenous peak lends further evidence of the composition of the CM being collagen due to collagen being the only material containing nitrogen during the fabrication process.

3.3 | FTIR

FTIR spectra from 1,700 to 1,000 cm^{-1} were acquired from six separate samples to determine the fibrilized nature of the CMs. The first sample tested was LC, which was added to the olive oil emulsion to form the CMs. The second sample was of the fibrilized collagen. To prepare the fibrilized collagen, LC was immersed in water for 24 hr to form a fibrilized collagen structure. The results, as shown in Figure 4, demonstrated that the fibrilized collagen and the CM samples had similar characteristic peaks. Collagen characteristic peaks were found at amide I between 1,700 and 1,600 cm^{-1}, amide II between 1,600 and 1,500 cm^{-1}, and amide III between 1,300 and 1,180 cm^{-1} corresponding to (C═O) stretching, (C—N) stretching and (N—H) bending, and (C—N) stretching, (C—H) bending, and (C—C) stretching (Belbachir, Noreen, Gouspillou, & Petibois, 2009).

While the CMs spectra mimic that of the fibrilized collagen's spectra with peaks found at the Amide I, Amide II, and Amide III absorption bands, the LC had two peaks at 1,585 and 1,400 cm^{-1} with a shoulder at 1630 cm^{-1}. After fibrillization of the collagen, the 1,585 and 1,400 cm^{-1} peaks are reduced and thereby revealing Amide I and Amide II absorption bands in the fibrilized collagen and CM samples.

3.4 | Cell viability

To evaluate the cellular toxicity of CMs fabricated in our study, we performed a WST-1 cell viability assay. We used CMs emulsified for 1- and 16-hr using 0.35% span-80. This study specifically helped determine if the CM emulsion time affected fibroblast cell viability over 7 days. CMs form after 1-hr of emulsion but we wanted to determine if CMs would eventually begin to denature at longer emulsion times and become less biocompatible. We chose to compare the 1-hr emulsion time with an emulsion time of 16-hr. L-929 fibroblast cells were incubated with the CMs at 3, 5, and 7 day time points. Untreated L-929 fibroblast cells were used as control. The results

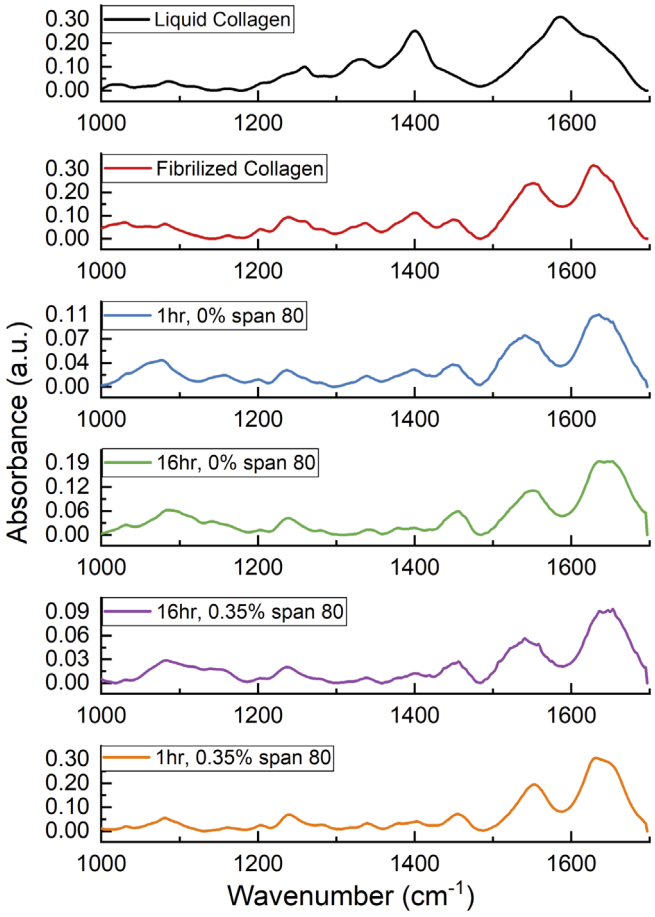

FIGURE 4 FTIR spectra of prefibrilized liquid collagen, fibrilized collagen, 1 hr emulsion CM with 0% span-80, 16-hr emulsion CM with 0% span-80, 16 hr emulsion CM with 0.35% span-80, and 1-hr emulsion CM with 0.35% span-80

demonstrated that there was no statistical significance between either group (1- or 16-hr emulsification time) relative to cells alone but inferences can be made upon the trend in cellular viability and visually how the cells interacted with the CMs during culture. After 3-days, as shown in Figure 5a, both the 1- and 16-hr CMs demonstrated equivalent cellular viability as compared to that of the control. Both Figure 5d,e show fibroblasts adhering to the surface of CMs. After 5 days, Figure 5b, both the 1- and 16-hr CMs showed overall increased viability in comparison to the control. Figure 5f,g showed significant coverage of fibroblast cells on the CMs with elongation of the fibroblasts extending from the CMs. At 7 days, Figure 5c, both 1- and 16-hr emulsions maintain a similar viability advantage in comparison to the control. Figure 5h,i shows a high density of fibroblasts covering the bottom of the well plate and complete coverage on the surface of CMs.

4 | DISCUSSION

Type I collagen is a triple helix, polypeptide chain protein that can be easily processed in a variety of forms. Processing collagen as an injectable fibrilized material for tissue engineering applications is advantageous not only due to collagen's excellent biocompatibility but also due to its ability to integrate with tissue in vivo, forming a template for cellular attachment and resulting in no harmful byproducts. However, the injectability of bulk collagen is problematic mainly due to its high viscosity; therefore, researchers have processed collagen in different forms such as microspheres to ease injectability. CMs are versatile materials but the limitations in terms of fabrication, such as the need for crosslinkers during emulsification and the limited ability to inject CMs fabricated using individual pipetting cycles, creates an opportunity to utilize LC to fabricate CMs. To overcome the limitations, we developed a simple, crosslinker free method to fabricate CMs with reproducibility for a wide range of musculoskeletal applications using LC.

Controlling the size of CMs during the fabrication process to create uniform size is critical for tissue engineering applications particularly if the CMs are entrapped with additional biomodulatory agents or cells. The release of biomodulatory agents and the survivability of cells can be controlled with greater accuracy relative to size uniformity in correlation to the release kinetics of a sphere. A wide range of CM sizes can result in a bulk release or delayed release of agents and thus may not achieve the therapeutic effect or even may result in cytotoxicity. In this study, we were able to better control the average diameter and standard deviation of the CMs by utilizing span-80. The use of span-80 resulted in a decreased CM diameter and standard deviation by decreasing the interfacial tension between water and oil (Matsuhashi et al., 2015). Figure 1 showed the influence of increasing concentrations of span-80 during the CM fabrication process. The increased concentration of span-80 proportionally led to a decrease in CM average diameter and standard deviation; however, CM spherical morphology was lost after increasing the span-80 concentration over 0.35%.

Evidence to support a collagenous fibrilized network within the CM was twofold. First, SEM imaging of 1- and 8-hr CM emulsions provided evidence of collagen fibrillization. The inspection of Figure 2a with the 1-hr emulsion time demonstrated a smooth surface. Uncovering the surface of the 1-hr emulsion CM using FIB milling, Figure 2b–f, provided evidence of a collagen network at the core of the CM. Through CPD in Figures 3a and 4b of an 8-hr emulsion CM, a collagenous network was visually apparent. An additional study was performed to verify the composition of CMs using EDS. EDS identified the elemental composition of an 8-hr CM emulsion on the surface as shown in Figure 3c. A nitrogenous peak was indicated on the surface of the CM. Nitrogen is a unique element to collagen during the CM fabrication process; thus further confirming the collagenous network created during fabrication.

The second method utilized to identify fibrilized collagen within the CM was FTIR analysis as shown in Figure 4. The FTIR scans of the CMs were compared to that of the LC and fibrilized collagen. The CMs scans mimicked that of fibrilized collagen scans, which indicates the fibrilized nature of the CMs. Characteristic peaks of collagen reported in literature also correlated with the peaks identified in the CM scans (Belbachir et al., 2009; de Campos & Mello, 2011; Payne & Veis, 1988). There were observable differences between the LC and the fibrilized collagen. For the LC, a single peak was identified at

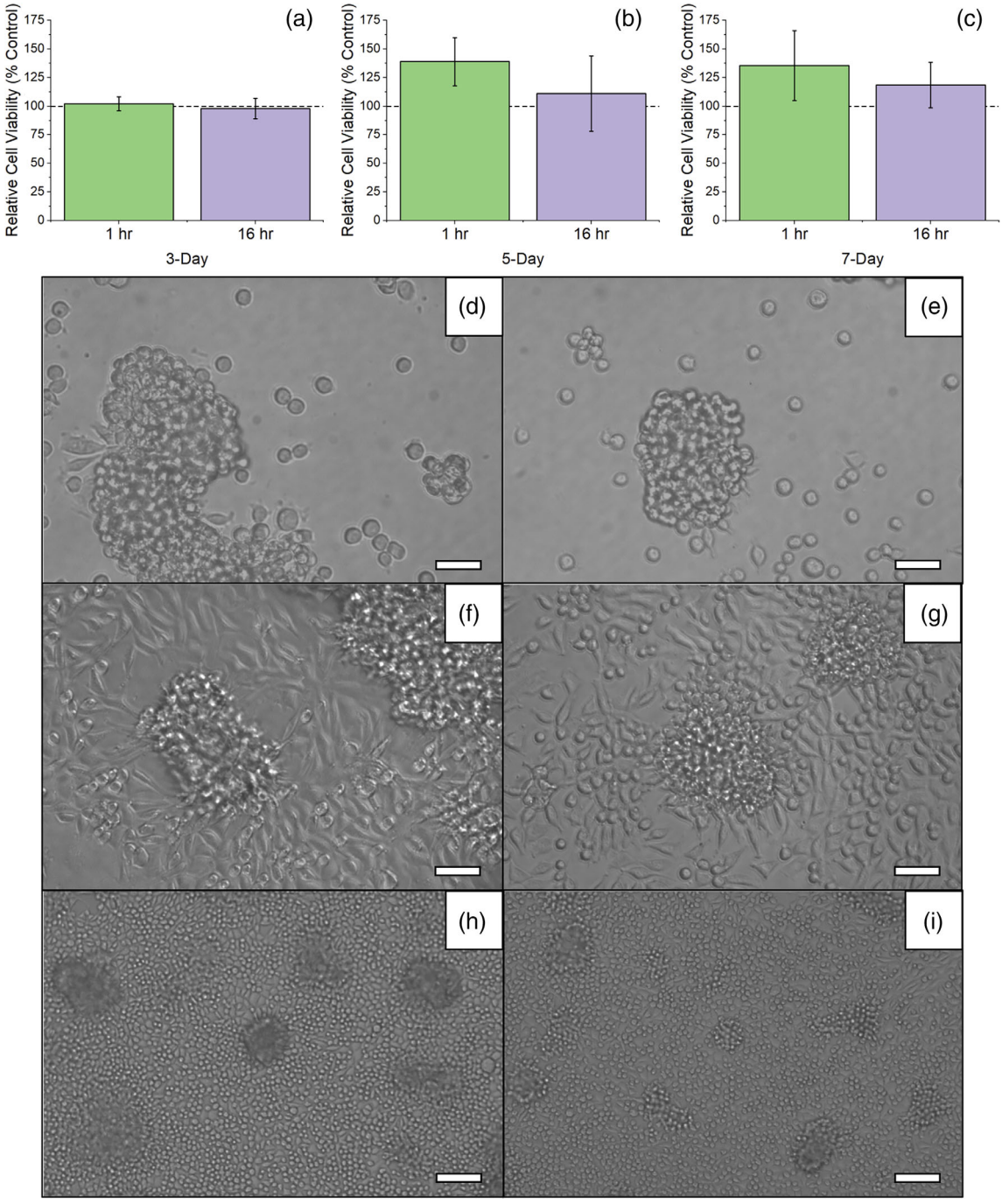

FIGURE 5 WST-1 cell viability assay with (a) 3-day, (b) 5-day, and (c) 7-day time points using L929 fibroblast cells. ×20 light microscope images of (d) 3-day 1-hr emulsion and 0.35% span-80, (e) 3-day 16-hr emulsion and 0.35% span-80, (f) 5-day 1-hr emulsion and 0.35% span-80, (g) 5-day 16-hr emulsion and 0.35% span-80. ×10 light microscope images of (h) 7-day 1-hr emulsion and 0.35% span-80, and (i) 7-day 16-hr emulsion and 0.35% span-80; Scale bar = 50 um

1,585 cm^{-1} while the fibrilized collagen and the CMs displayed two individual peaks at 1,635 cm^{-1} and 1,545 cm^{-1}, which corresponded to amide I and amide II respectively. Also, the LC sample had a significant peak at 1,400 cm^{-1} relative to all other samples. The literature suggests that a peak at 1,400 cm^{-1} is attributed to CH_2 bending from glycine residues and also symmetrical stretching of (COO—) from glutamate and aspartate (Barth, 2000; Boryskina, Bolbukh, Semenov, Gasan, & Maleev, 2007; Parikh et al., 2011) found in LC. Liu et al. proposed the diminishment in the intensity of 1,400 cm^{-1} may be due to dehydration of Type I collagen during the crosslinking or fibrillization stage (Boryskina et al., 2007; Liu et al., 2013). Fibrillization of collagen leads to dehydration (Miles, Avery, Rodin, & Bailey, 2005). It was observed that our CMs demonstrated a decrease in the 1,400 cm^{-1} peak, which can be attributed to fibrillization; helps to validate the fibrillization of the CMs.

It was imperative that the CMs demonstrated biocompatibility. Cellular viability was performed to determine the compatibility of CMs with L-929 fibroblast cells. Three, five, and seven-day time points were evaluated and compared between the 1- and 16-hr CM emulsion times. At 3 days, both the 1- and 16-hr CM emulsions were equivalent in cellular viability to the negative control (Figure 5a). At Days 5 and 7, there was an overall trend toward enhanced viability compared to the negative control by both 1- and 16-hr CM emulsions (Figure 5d–g). Upon visual inspection of the cells and the CMs over 7 days, it appeared that the cells have an attraction toward the CMs. As shown in Figure 5d–i, cells were more clustered on the CMs than on the bottom of the 96-well plate. The CMs may play a role in enhancing cellular proliferation. While no quantitative data was recorded, the cells appeared to wrap around the surface of the CMs and gave the appearance of being adherent to the surface of the CMs. The cells also appeared to be extending from the CMs and creating a cellular network. These results were similarly observed by Matsuhashi et al. (2015) when incubating CMs with NIH3T3 cells.

Our findings demonstrated that fibroblast cells have an affinity for the crosslinker-free CMs. The cells may be experiencing a native-like recognition and cell attachment due to a larger number of integrin moieties of the Type I collagen along with a more open network relative to work using various chemical crosslinking agents (Bax et al., 2017; Grover et al., 2012). In future work, we propose the use of CMs as possible bioactive agent carriers and cell transporters. With extensive work performed looking into adipose-derived mesenchymal stem cells (ADSC) on chondrocyte cells and on the differentiation into chondrocyte cells we feel that CMs are uniquely suited as an injectable transporter for ADSCs into osteoarthritc tissues due to their injectable size and their affinity core cellular adherence (Barlian, Judawisastra, Alfarafisa, Wibowo, & Rosadi, 2018; Manferdini et al., 2013; Zhou et al., 2019). We would like to look at the integration of CMs and ADSCs in a traditional impeller bioreactor and look into the effect of CM-ADSCs on osteoarthritic chondrocyte cells or CM-differentiated ADSCs into chondrocyte cells on osteoarthric articular cartilage.

5 | CONCLUSION

In this study, we developed a crosslinker-free method to fabricate CMs. CMs were developed using a LC in a water-in-oil emulsion process. We were able to modify the size of the CMs by using span-80. Fibrilized CM structures were studied for up to 16-hr emulsion times. The spherical and fibrilized nature was confirmed via SEM. EDS analysis confirmed CMs composition through the identification of a unique nitrogenous peak to collagen. FTIR analysis also confirmed collagen transitioning from a prefibrilized state prior to the emulsion and subsequently to a fibrilized state after emulsion. The CMs exhibited biocompatibility for both 1- and 16-hr emulsion times and it appeared that the cells preferentially adhered to the CMs. This crosslinker-free method to fabricate CMs resulted in spherical, stable, biocompatible CMs. The applications could include injectable delivery agents for biomodulatory molecules or cellular transporter to achieve self-assembled scaffolds for tissue recapitulation.

REFERENCES

Barlian, A., Judawisastra, H., Alfarafisa, N. M., Wibowo, U. A., & Rosadi, I. (2018). Chondrogenic differentiation of adipose-derived mesenchymal stem cells induced by L-ascorbic acid and platelet rich plasma on silk fibroin scaffold. *PeerJ*, *6*, e5809–e5809.

Barth, A. (2000). The infrared absorption of amino acid side chains. *Progress in Biophysics and Molecular Biology*, *74*(3), 141–173.

Bax, D. V., Davidenko, N., Gullberg, D., Hamaia, S. W., Farndale, R. W., Best, S. M., & Cameron, R. E. (2017). Fundamental insight into the effect of carbodiimide crosslinking on cellular recognition of collagen-based scaffolds. *Acta Biomaterialia*, *49*, 218–234.

Belbachir, K., Noreen, R., Gouspillou, G., & Petibois, C. (2009). Collagen types analysis and differentiation by FTIR spectroscopy. *Analytical and Bioanalytical Chemistry*, *395*(3), 829–837.

Bella, J., Eaton, M., Brodsky, B., & Berman, H. M. (1994). Crystal and molecular structure of a collagen-like peptide at 1.9 a resolution. *Science*, *266*(5182), 75–81.

Boryskina, O. P., Bolbukh, T. V., Semenov, M. A., Gasan, A. I., & Maleev, V. Y. (2007). Energies of peptide–peptide and peptide–water hydrogen bonds in collagen: Evidences from infrared spectroscopy, quartz piezogravimetry and differential scanning calorimetry. *Journal of Molecular Structure*, *827*(1), 1–10.

Chan, O., So, K.-F., & Chan, B. (2008). Fabrication of nano-fibrous collagen microspheres for protein delivery and effects of photochemical crosslinking on release kinetics. *Journal of Controlled Release*, *129*(2), 135–143.

Chen, J.-P., Chang, G.-Y., & Chen, J.-K. (2008). Electrospun collagen/chitosan nanofibrous membrane as wound dressing. *Colloids and Surfaces A: Physicochemical and Engineering Aspects*, *313*, 183–188.

Chowdhury, D. K., & Mitra, A. K. (1999). Kinetics of in vitro release of a model nucleoside deoxyuridine from crosslinked insoluble collagen and collagen–gelatin microspheres. *International Journal of Pharmaceutics*, *193*(1), 113–122.

de Campos, V. B., & Mello, M. L. S. (2011). Collagen type I amide I band infrared spectroscopy. *Micron*, *42*(3), 283–289.

Devore, D., Zhu, J., Brooks, R., McCrate, R. R., Grant, D. A., & Grant, S. A. (2016). Development and characterization of a rapid polymerizing collagen for soft tissue augmentation. *Journal of Biomedical Materials Research Part A*, *104*(3), 758–767.

Glowacki, J., & Mizuno, S. (2008). Collagen scaffolds for tissue engineering. *Biopolymers*, *89*(5), 338–344.

Gough, J. E., Scotchford, C. A., & Downes, S. (2002). Cytotoxicity of glutaraldehyde crosslinked collagen/poly (vinyl alcohol) films is by the mechanism of apoptosis. *Journal of Biomedical Materials Research*, *61*(1), 121–130.

Grover, C. N., Gwynne, J. H., Pugh, N., Hamaia, S., Farndale, R. W., Best, S. M., & Cameron, R. E. (2012). Crosslinking and composition influence the surface properties, mechanical stiffness and cell reactivity of collagen-based films. *Acta Biomaterialia*, *8*(8), 3080–3090.

Li, Y. Y., Cheng, H. W., Cheung, K. M. C., Chan, D., & Chan, B. P. (2014). Mesenchymal stem cell-collagen microspheres for articular cartilage repair: Cell density and differentiation status. *Acta Biomaterialia*, *10*(5), 1919–1929.

Liu, J., Lin, H., Li, X., Fan, Y., & Zhang, X. (2015). Chondrocytes behaviors within type I collagen microspheres and bulk hydrogels: An in vitro study. *RSC Advances*, *5*(67), 54446–54453.

Liu, Y., Chen, M., Yao, X., Xu, C., Zhang, Y., & Wang, Y. (2013). Enhancement in dentin collagen's biological stability after proanthocyanidins treatment in clinically relevant time periods. *Dental Materials*, *29*(4), 485–492.

Manferdini, C., Maumus, M., Gabusi, E., Piacentini, A., Filardo, G., Peyrafitte, J. A., … Facchini, A. (2013). Adipose-derived mesenchymal

stem cells exert antiinflammatory effects on chondrocytes and synoviocytes from osteoarthritis patients through prostaglandin E2. *Arthritis and Rheumatism*, *65*(5), 1271–1281.

Mathieu, M., Vigier, S., Labour, M., Jorgensen, C., Belamie, E., & Noël, D. (2014). Induction of mesenchymal stem cell differentiation and cartilage formation by cross-linker-free collagen microspheres. *European Cells & Materials*, *28*, 82–96.

Matsuhashi, A., Nam, K., Kimura, T., & Kishida, A. (2015). Fabrication of fibrillized collagen microspheres with the microstructure resembling an extracellular matrix. *Soft Matter*, *11*(14), 2844–2851.

Miles, C. A., Avery, N. C., Rodin, V. V., & Bailey, A. J. (2005). The increase in denaturation temperature following cross-linking of collagen is caused by dehydration of the Fibres. *Journal of Molecular Biology*, *346*(2), 551–556.

Mozdzen, L. C., Rodgers, R., Banks, J. M., Bailey, R. C., & Harley, B. A. (2016). Increasing the strength and bioactivity of collagen scaffolds using customizable arrays of 3D-printed polymer fibers. *Acta Biomaterialia*, *33*, 25–33.

Mumcuoglu, D., de Miguel, L., Jekhmane, S., Siverino, C., Nickel, J., Mueller, T. D., … Kluijtmans, S. G. (2018). Collagen I derived recombinant protein microspheres as novel delivery vehicles for bone morphogenetic protein-2. *Materials Science and Engineering: C*, *84*, 271–280.

Nagai, N., Kumasaka, N., Kawashima, T., Kaji, H., Nishizawa, M., & Abe, T. (2010). Preparation and characterization of collagen microspheres for sustained release of VEGF. *Journal of Materials Science: Materials in Medicine*, *21*(6), 1891–1898.

Parenteau-Bareil, R., Gauvin, R., & Berthod, F. (2010). Collagen-based biomaterials for tissue engineering applications. *Materials*, *3*(3), 1863–1887.

Parikh, S. J., Kubicki, J. D., Jonsson, C. M., Jonsson, C. L., Hazen, R. M., Sverjensky, D. A., & Sparks, D. L. (2011). Evaluating glutamate and aspartate binding mechanisms to rutile (α-TiO2) via ATR-FTIR spectroscopy and quantum chemical calculations. *Langmuir*, *27*(5), 1778–1787.

Payne, K., & Veis, A. (1988). Fourier transform IR spectroscopy of collagen and gelatin solutions: Deconvolution of the amide I band for conformational studies. *Biopolymers*, *27*(11), 1749–1760.

Savolainen, J., Väänänen, K., Puranen, J., Takala, T., Komulainen, J., & Vihko, V. (1988). Collagen synthesis and proteolytic activities in rat skeletal muscles: Effect of cast-immobilization in the lengthened and shortened positions. *Archives of Physical Medicine and Rehabilitation*, *69*(11), 964–969.

Shoulders, M. D., & Raines, R. T. (2009). Collagen structure and stability. *Annual Review of Biochemistry*, *78*, 929–958.

Sung, H.-W., Huang, R.-N., Huang, L. L., & Tsai, C.-C. (1999). In vitro evaluation of cytotoxicity of a naturally occurring cross-linking reagent for biological tissue fixation. *Journal of Biomaterials Science, Polymer Edition*, *10*(1), 63–78.

Uzman, A. (2001). Molecular cell biology (4th edition) Harvey Lodish, Arnold Berk, S. Lawrence Zipursky, Paul Matsudaira, David Baltimore and James Darnell; Freeman & co., New York, NY, 2000, 1084 pp., list price $102.25, ISBN 0-7167-3136-3. *Biochemistry and Molecular Biology Education*, *29*(3), 126–128.

Wu, T.-J., Huang, H.-H., Lan, C.-W., Lin, C.-H., Hsu, F.-Y., & Wang, Y.-J. (2004). Studies on the microspheres comprised of reconstituted collagen and hydroxyapatite. *Biomaterials*, *25*(4), 651–658.

Yang, C., & Wang, J. (2014). Preparation and characterization of collagen microspheres for sustained release of steroidal saponins. *Materials Research*, *17*(6), 1644–1650.

Yuan, M., Leong, K. W., & Chan, B. P. (2011). Three-dimensional culture of rabbit nucleus pulposus cells in collagen microspheres. *The Spine Journal*, *11*(10), 947–960.

Zhou, J., Wang, Y., Liu, Y., Zeng, H., Xu, H., & Lian, F. (2019). Adipose derived mesenchymal stem cells alleviated osteoarthritis and chondrocyte apoptosis through autophagy inducing. *Journal of Cellular Biochemistry*, *120*(2), 2198–2212.

How to cite this article: Snider C, Bellrichard M, Meyer A, Kannan R, Grant D, Grant S. A novel crosslinker-free technique toward the fabrication of collagen microspheres. *J Biomed Mater Res*. 2020;108B:2789–2798. https://doi.org/10.1002/jbm.b.34608